Electronic Supplementary Material (ESI) for Energy & Environmental Science.

Supplementary Information

A Facile Strategy for Third Component Selection in Non-Fullerene Acceptor Based Ternary Organic Solar Cells

Yun Li,‡[a] Yunhao Cai,‡*[a] Yuanpeng Xie,[a] Junhua Song,[a] Hongbo Wu,[b] Zheng Tang,[b] Jie Zhang,[c] Fei Huang,[c] and Yanming Sun*[a]

Y. Li, Dr. Y. Cai, Dr. Y. Xie, J. Song, Prof. Y. Sun
School of Chemistry
Beihang University
Beijing 100191, P. R. China
E-mail: caiyunhao@buaa.edu.cn; sunym@buaa.edu.cn

H. Wu, Prof. Z. Tang
State Key Laboratory for Modification of Chemical Fibers and Polymer Materials, Center for Advanced Low-dimension Materials, College of Materials Science and Engineering, Donghua University Shanghai, 201620, P. R. China

Dr. J. Zhang, Prof. F. Huang
State Key Laboratory of Luminescent Materials and Devices, South China University of Technology, Guangzhou 510640, P. R. China,

‡ Y. Li and Y. Cai contributed equally to this work.

Materials

PM6 was purchased from Solarmer Inc. D18-Cl was purchased from eFlexPV Limited. BTP-eC9 and Y6 was purchased from hyperchemical Inc. L8-BO and L8-BO-F was synthesized in our group according to previously reported literature.[1,2]

Unless otherwise noted, all reagents and chemicals were purchased from commercial sources and used without further purification. Anhydrous THF was distilled from sodium/benzophenoneketyl prior to use. 12,13-bis(2-butyloctyl)-3,9-dinonyl-12,13-dihydro-[1,2,5]thiadiazolo[3,4-e]thieno[2",3":4',5']thieno[2',3':4,5]pyrrolo[3,2-g]thieno[2',3':4,5]thieno[3,2-b]indole-2,10-dicarbaldehyde and 12,13-bis(2-ethylhexyl)-3,9-diundecyl-12,13-dihydro-[1,2,5]thiadiazolo[3,4-e]thieno[2",3":4',5']thieno[2',3':4,5]pyrrolo[3,2-g]thieno[2',3':4,5]thieno[3,2-b]indole-2,10-dicarbaldehyde were synthesized according to previously reported literature.[3-5]

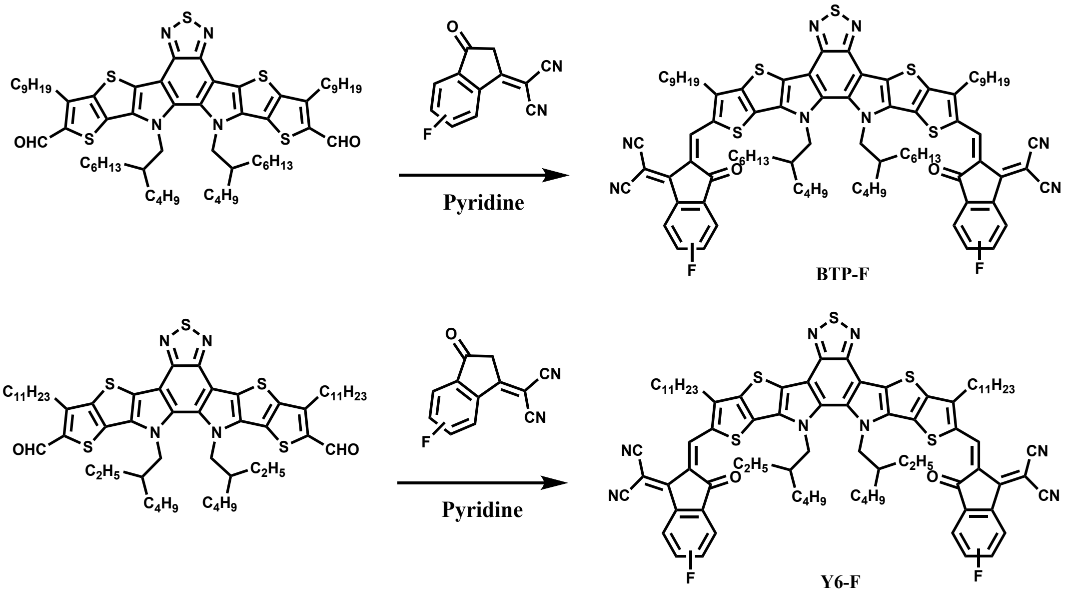

Scheme S1. Synthetic routes of BTP-F and Y6-F.

To a 100 mL two-necked round-bottomed flask was charged sequentially with 3,9-bis(2-butyloctyl)-12,13-bis(2-ethylhexyl)-12,13-dihydro-[1,2,5]thiadiazolo[3,4-e]thieno[2'',3'':4',5']thieno[2',3':4,5]pyrrolo[3,2-g]thieno[2',3':4,5]thieno[3,2-b]indole-2,10-dicarbaldehyde (120 mg, 0.110 mmol, 1 equiv), 2-(5-fluoro-3-oxo-2,3-dihydro-1H-inden-1-ylidene)malononitrile and 2-(6-fluoro-3-oxo-2,3-dihydro-1H-inden-1-ylidene)malononitrile mixture (54 mg, 0.254 mmol, 2.3 equiv) and $CHCl_3$ (30 mL). After the reaction mixture was stirred at room temperature for 10 min under protection of nitrogen, pyridine (0.5 mL) was added and the reaction was stirred at 55 °C for 4 hours. After removal of the solvent under vacuum, the residue was purified by column chromatography on silica gel with petroleum ether: dichloromethane (2:3, v: v) as an eluent to yield an isolated BTP-F as a black solid (133 mg, 81.5%). For BTP-F: 1H NMR (400 MHz, $CDCl_3$) : δ 9.16 (s, 2H), 8.72 (m, 0.57H), 8.41 (m, 1.38H), 7.96 (m, 1.40H), 7.57 (m, 0.57H), 7.43 (m, 2H), 4.78 (m, 4H), 3.23 (m, 4H), 2.15 (m, 2H), 1.90 (m, 4H), 1.57 (s, 2H), 1.55 (m, 4H), 1.39 (m, 4H), 1.28 (m, 20H), 0.98 (m, 18H), 0.89 (m, 10H), 0.65 (m, 14H), 0.07 (S, 2H). MALDI-TOF (m/z) calculated for $C_{86}H_{94}F_2N_8O_2S_5$ [M] $^+$:1470.62, found: 1470.7.

To a 100 mL two-necked round-bottomed flask was charged sequentially with 12,13-bis(2-ethylhexyl)-3,9-diundecyl-12,13-dihydro-[1,2,5]thiadiazolo[3,4-e]thieno[2'',3'':4',5']thieno[2',3':4,5]pyrrolo[3,2-g]thieno[2',3':4,5]thieno[3,2-b]indole-2,10-dicarbaldehyde (100 mg, 0.097 mmol, 1 equiv), 2-(5-fluoro-3-oxo-2,3-dihydro-1H-inden-1-ylidene)malononitrile and 2-(6-fluoro-3-oxo-2,3-dihydro-1H-inden-1-ylidene)malononitrile mixture (44.5 mg, 0.195 mmol, 2.3 equiv) and $CHCl_3$ (30 mL). After the reaction mixture was stirred at room temperature for 10 min under protection of nitrogen, pyridine (0.5 mL) was added and the reaction was stirred at 55 ºC for 4 hours. After removal of the solvent under vacuum, the residue was purified by column chromatography on silica gel with petroleum ether: dichloromethane (2:3, v:v) as an eluent to yield an isolated BTP-eC9F as a black solid (112 mg, 80.5%). For Y-F: ^{1}H NMR (600 MHz, $CDCl_3$) δ 9.14 (d, J = 7.3 Hz, 2H), 8.72 (m, 0.47H), 8.38 (m, 1.45H), 7.96 (m, 1.47H), 7.60 (m, 0.47H), 7.43 (m, 2H), 4.79 (m, 4H), 3.22 (m, 4H), 2.13 (m, 2H), 1.87 (m, 4H), 1.60 (s, 6H), 1.51 (m, 4H), 1.37 (m, 4H), 1.25 (m, 38H), 1.05 (m, 10H), 0.87 (m, 6H), 0.76 (m, 6H), 0.66 (m, 6H).[5]

Materials Characterization

The nuclear magnetic resonance (NMR) spectra were recorded on a Bruker Avance 400 MHz and 600 MHz spectrometer with deuterated chloroform ($CDCl_3$) and trimethylsilane (TMS) as the solvent and internal reference, respectively. The mass spectra were measured using Bruker Daltonics Biflex III MALDI-TOF Analyzer in the MALDI mode.

Measurements and Characterizations

UV-vis absorption spectra of the pristine and blend films were acquired with a UV-vis spectrophotometer (Shimadzu UV-3700). Cyclic voltammetry (CV) measurements was performed on a CHI660E electrochemical workstation in a three-electrode cell in anhydrous acetonitrile solvents solution of Bu_4NPF^6 (0.1 M) with a scan rate of 50 mV/s at room temperature under argon. A Ag/Ag^+ wire, two platinum wires were used as the reference electrode, counter electrode, and working electrode, respectively. The materials to be tested in chloroform solution were dried on the surface of the working electrode. The potential of Ag/Ag^+ reference electrode was internally calibrated by using ferrocene/ ferrocenium (Fc/Fc^+) as the redox couple. The water and glycerol contact angle images of neat films were recorded by using a KRÜSS DSA 100 instrument under atmospheric condition. DSC measurements were performed on the PerkinElmer Diamond DSC instrument with a heating rate of 10 ºC min^{-1} under nitrogen atmosphere. Device current density-voltage (J-V) characteristics were recorded using a Keithley 2400 Source Measure Unit. The photocurrent was tested under AM 1.5G illumination at 100 $mWcm^{-2}$ using a solar simulator (Class AAA solar simulator, Model 94063A, Oriel). The light intensity was calibrated using a standard Si solar cell and a readout meter (Model 91150V, Newport). The mobility was determined by fitting the dark current to the model of a single carrier SCLC, according to the equation: $J = 9\varepsilon_0\varepsilon_r\mu V^2/8d^3$, where J is the current density, d is the film thickness of the active layer, μ is the charge carrier mobility, ε_r is the relative dielectric constant of the transport medium, and ε_0 is the permittivity of free space. The carrier mobility can be calculated from the slope of the $J^{0.5} \sim V$ curves. The electroluminescence (EL) spectra were taken using a

Kymera-328I spectrograph and an EMCCD purchased from Andor Technology (DU970P). Injection current used for EL was 1 mA cm^{-2}. EQE$_{EL}$ measurements were performed using a home-built setup using a Keithley 2400 to inject current to the solar cells. Emission photon-flux from the solar cells was recorded using a Si detector (Hamamatsu s1337-1010BQ) and a Keithley 6482 picoammeter. Sensitive EQE measurements were done using a halogen lamp light source, chopped at a frequency of 173 Hz, a monochromator (Newport CS260), a Stanford SR830 lock-in amplifier, a Stanford SR570 current amplifier, and a set of long pass filters. Lamp intensity was calibrated using a Si detector (Hamamatsu s1337-1010BQ). AFM measurement was performed on a Dimension Icon AFM (Bruker) in a tapping mode under ambient conditions. Grazing incidence wide-angle X-ray scattering (GIWAXS) patterns were acquired by detector Pilatus3R 1M, Dectris (X-ray Source: MetalJet-D2, Excillum).

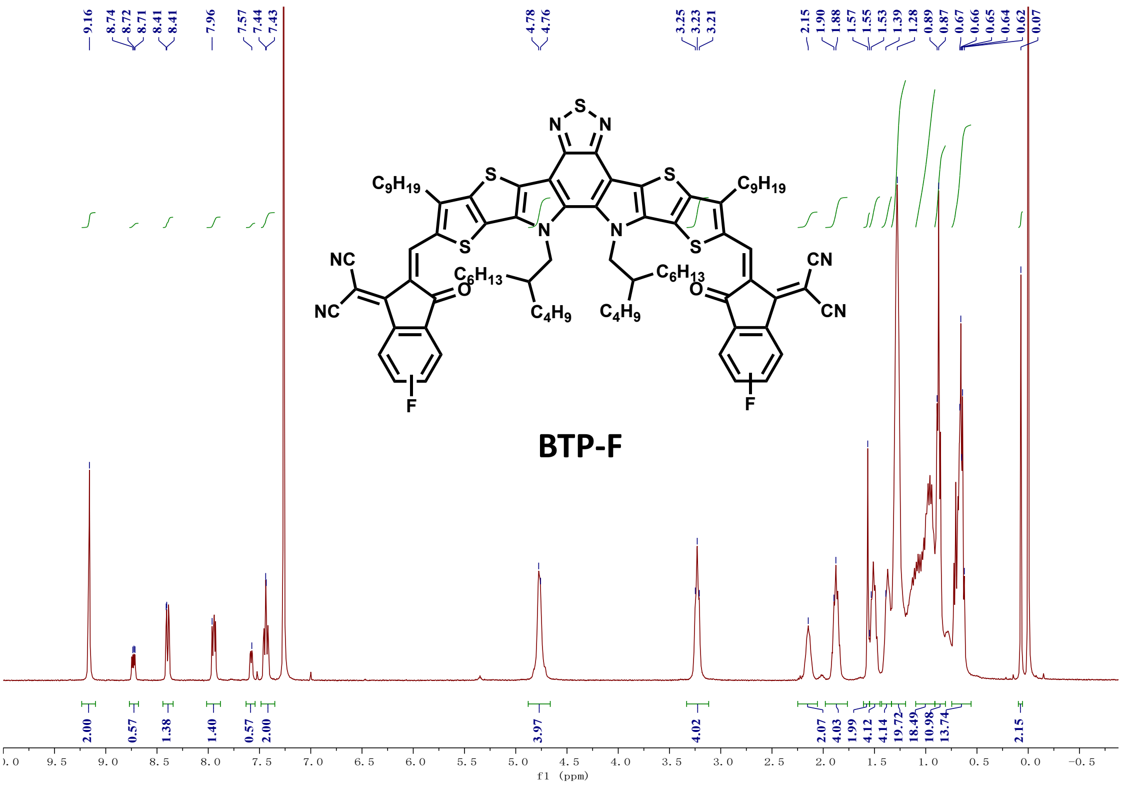

BTP-F

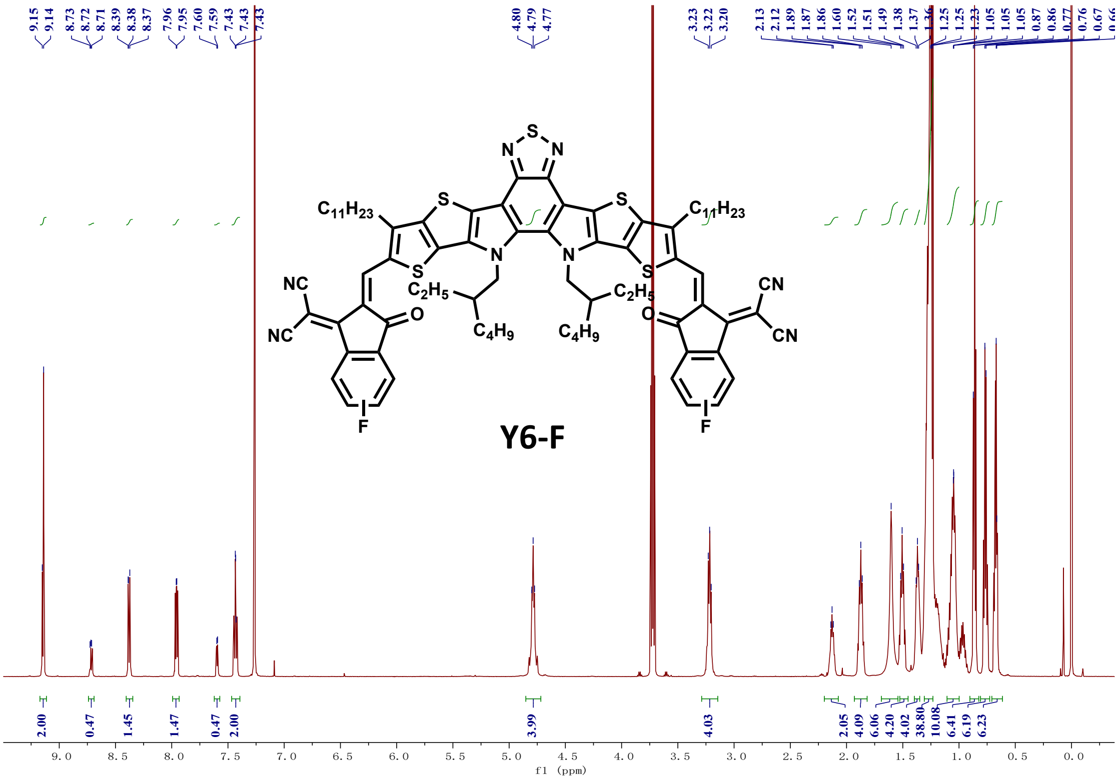

Fig. S1 ^{1}H NMR spectra of BTP-F and Y6-F.

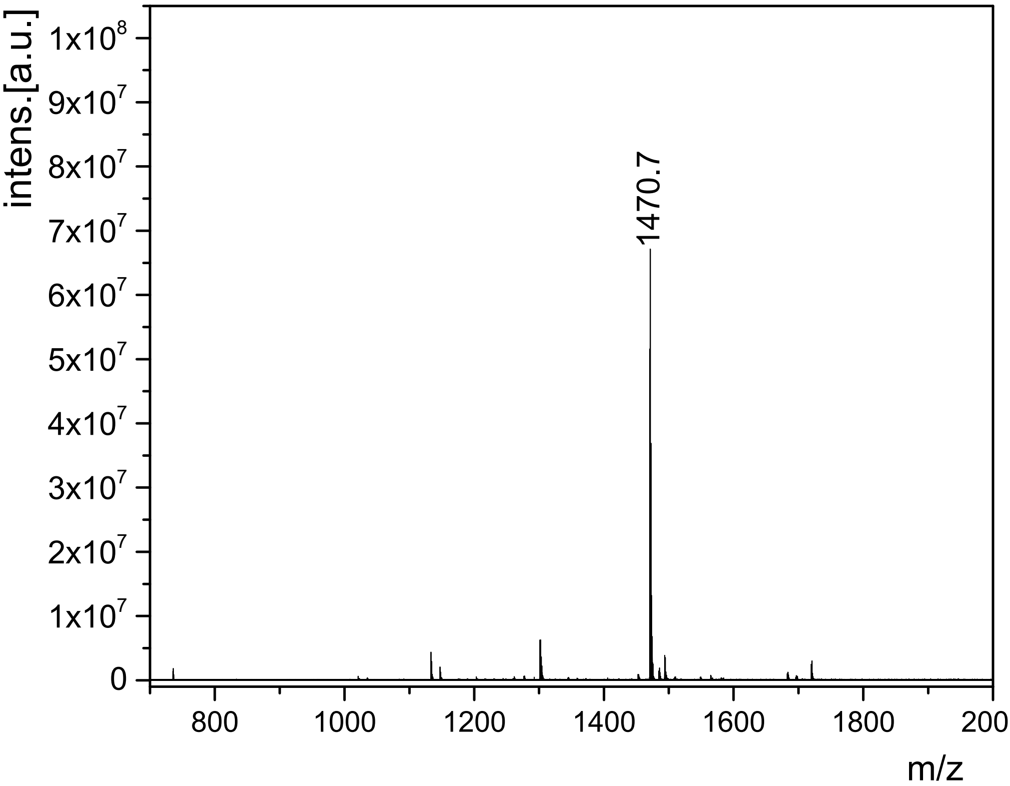

Fig. S2 MALDI-TOF spectrum of BTP-F.

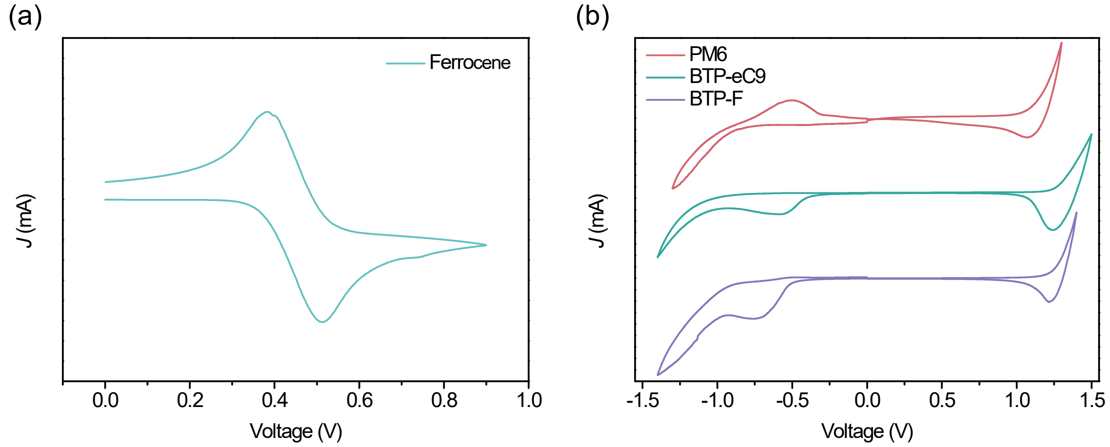

Fig. S3 Current-voltage curves of cyclic voltammetry (CV) measurements of ferrocene (a) and PM6, BTP-eC9, and BTP-F (b).

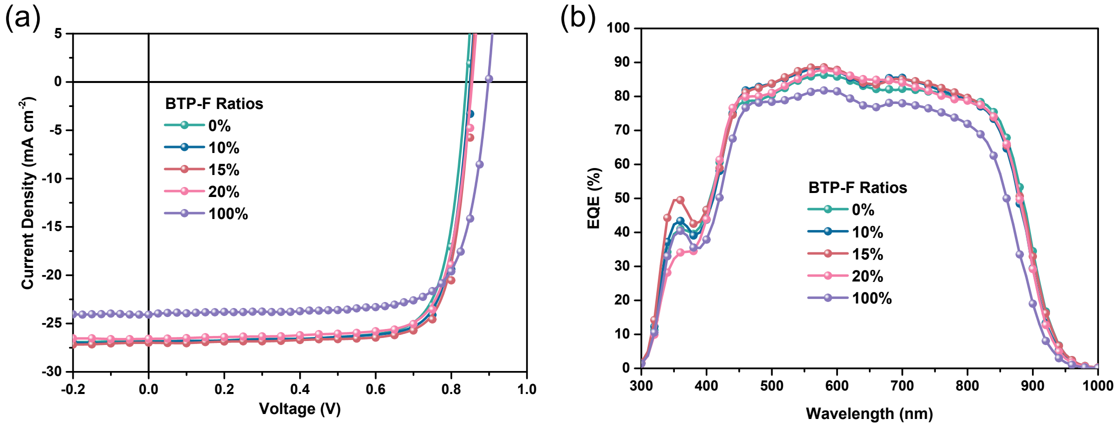

Fig. S4 (a) Current-voltage (*J-V*) curves of PM6:BTP-eC9:BTP-F devices with different BTP-F contents under AM 1.5 G solar irradiation (100 mW cm^{-2}) and (b) the corresponding EQE spectra.

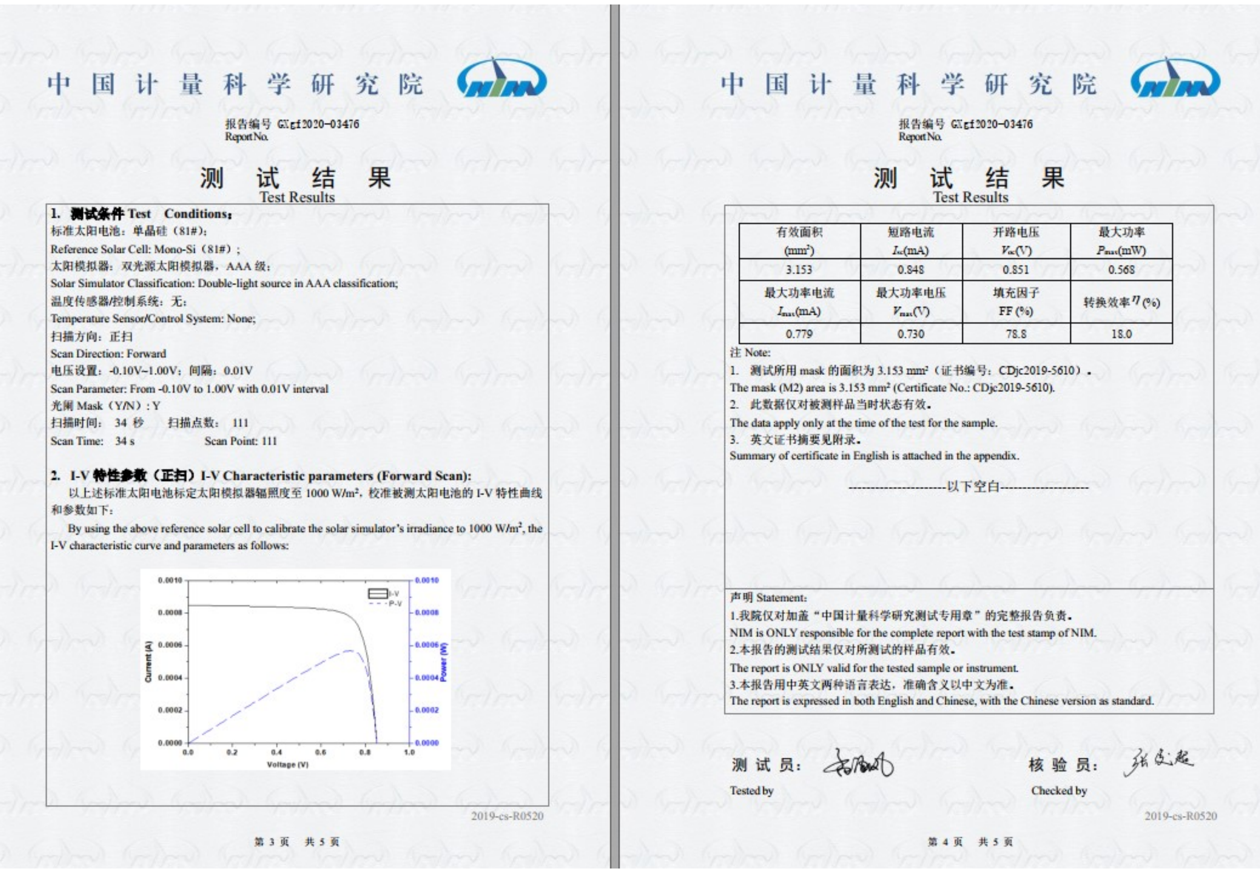
中国计量科学研究院

报告编号 GXgf2020-03476
Report No.

测试结果
Test Results

1. 测试条件 Test Conditions:
标准太阳电池：单晶硅（81#）；
Reference Solar Cell: Mono-Si（81#）；
太阳模拟器：双光源太阳模拟器，AAA 级；
Solar Simulator Classification: Double-light source in AAA classification;
温度传感器/控制系统：无；
Temperature Sensor/Control System: None;
扫描方向：正扫
Scan Direction: Forward
电压设置：-0.10V~1.00V；间隔：0.01V
Scan Parameter: From -0.10V to 1.00V with 0.01V interval
光阑 Mask（Y/N）: Y
扫描时间： 34 秒　扫描点数： 111
Scan Time: 34 s　Scan Point: 111

2. I-V 特性参数（正扫）I-V Characteristic parameters (Forward Scan):

以上述标准太阳电池标定太阳模拟器辐照度至 1000 W/m²，校准被测太阳电池的 I-V 特性曲线和参数如下：

By using the above reference solar cell to calibrate the solar simulator's irradiance to 1000 W/m², the I-V characteristic curve and parameters as follows:

2019-cs-R0520

第 3 页　共 5 页

中国计量科学研究院

报告编号 GXgf2020-03476
Report No.

测试结果
Test Results

有效面积 (mm²)	短路电流 I_{sc}(mA)	开路电压 V_{oc}(V)	最大功率 P_{max}(mW)
3.153	0.848	0.851	0.568
最大功率电流 I_{max}(mA)	最大功率电压 V_{max}(V)	填充因子 FF (%)	转换效率 η (%)
0.779	0.730	78.8	18.0

注 Note:
1. 测试所用 mask 的面积为 3.153 mm²（证书编号：CDjc2019-5610）。
The mask (M2) area is 3.153 mm² (Certificate No.: CDjc2019-5610).
2. 此数据仅对被测样品当时状态有效。
The data apply only at the time of the test for the sample.
3. 英文证书摘要见附录。
Summary of certificate in English is attached in the appendix.

---------------------以下空白-------------------

声明 Statement:
1.我院仅对加盖“中国计量科学研究测试专用章”的完整报告负责。
NIM is ONLY responsible for the complete report with the test stamp of NIM.
2.本报告的测试结果仅对所测试的样品有效。
The report is ONLY valid for the tested sample or instrument.
3.本报告用中英文两种语言表达，准确含义以中文为准。
The report is expressed in both English and Chinese, with the Chinese version as standard.

测试员：
Tested by

核验员：
Checked by

2019-cs-R0520

第 4 页　共 5 页

Fig. S5 Report of the certified efficiency of PM6:BTP-eC9:BTP-F ternary device at National Institute of Metrology, China.

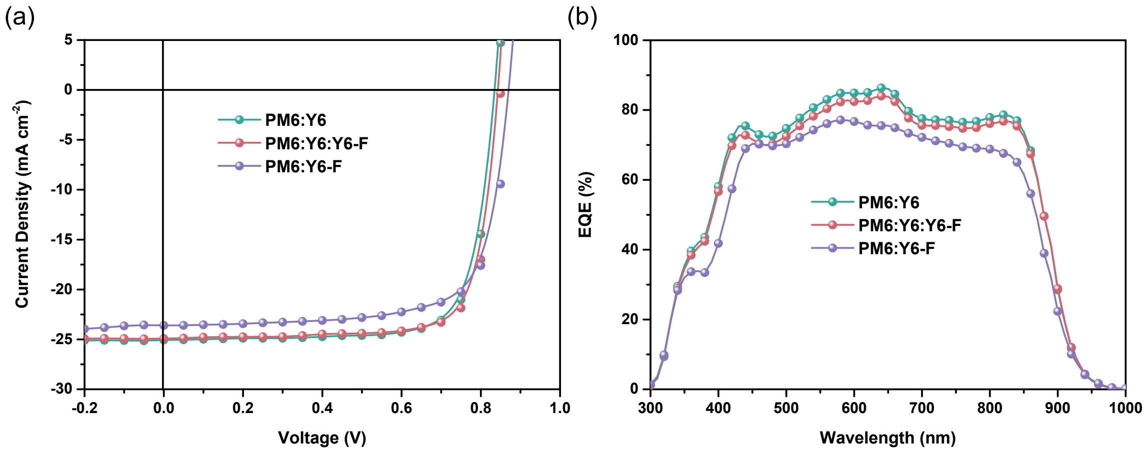

Fig. S6 (a) Current-voltage (*J-V*) curves of PM6:Y6, PM6:Y6-F, and PM6:Y6:Y6-F devices under AM 1.5 G solar irradiation (100 mW cm^{-2}) and (b) the corresponding EQE spectra.

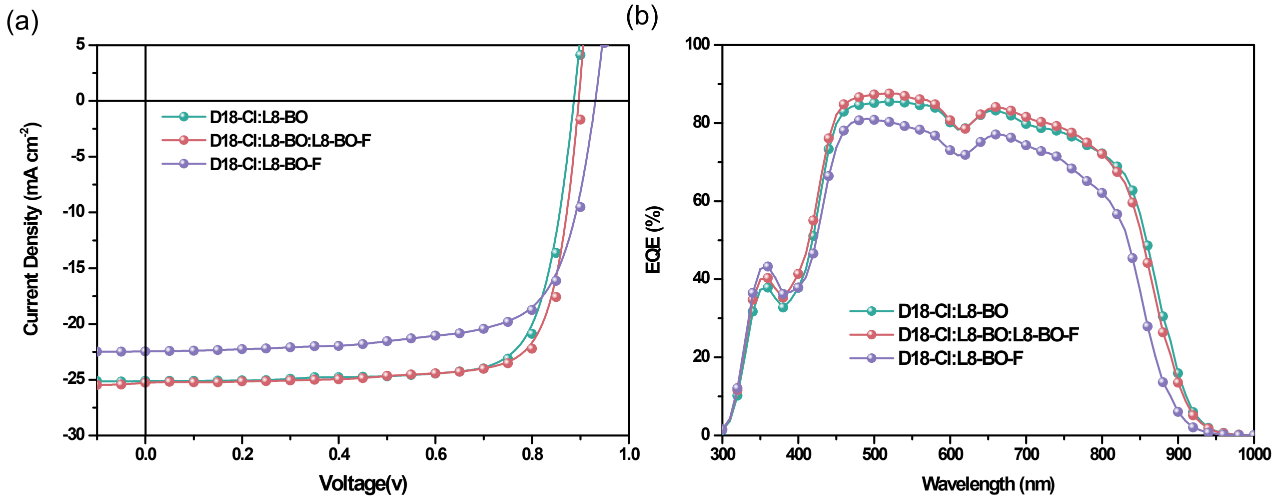

Fig. S7 (a) Current-voltage (*J-V*) curves of D18-Cl:L8-BO, D18-Cl:L8-BO-F and D18-Cl:L8-BO:L8-BO-F devices under AM 1.5 G solar irradiation (100 mW cm^{-2}) and (b) the corresponding EQE spectra.

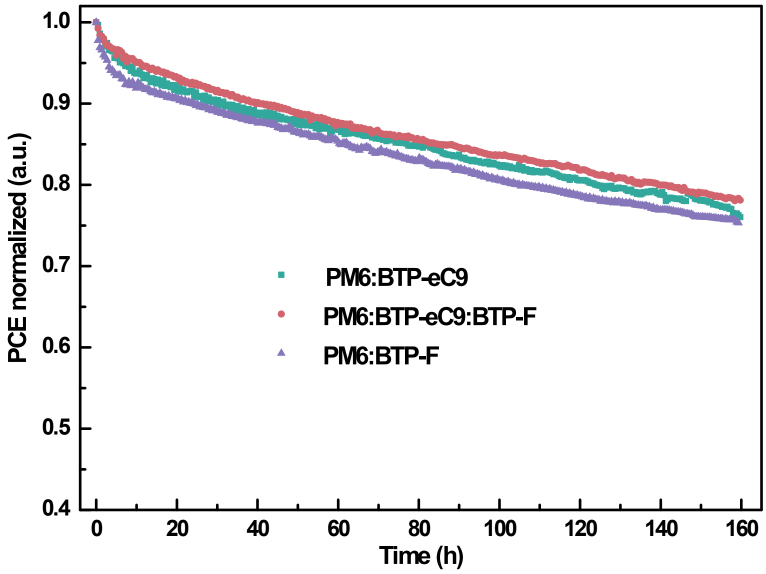

Fig. S8 Photostability test of the binary and ternary devices from maximum power point tracking under continuous illumination equivalent to ~1 sun.

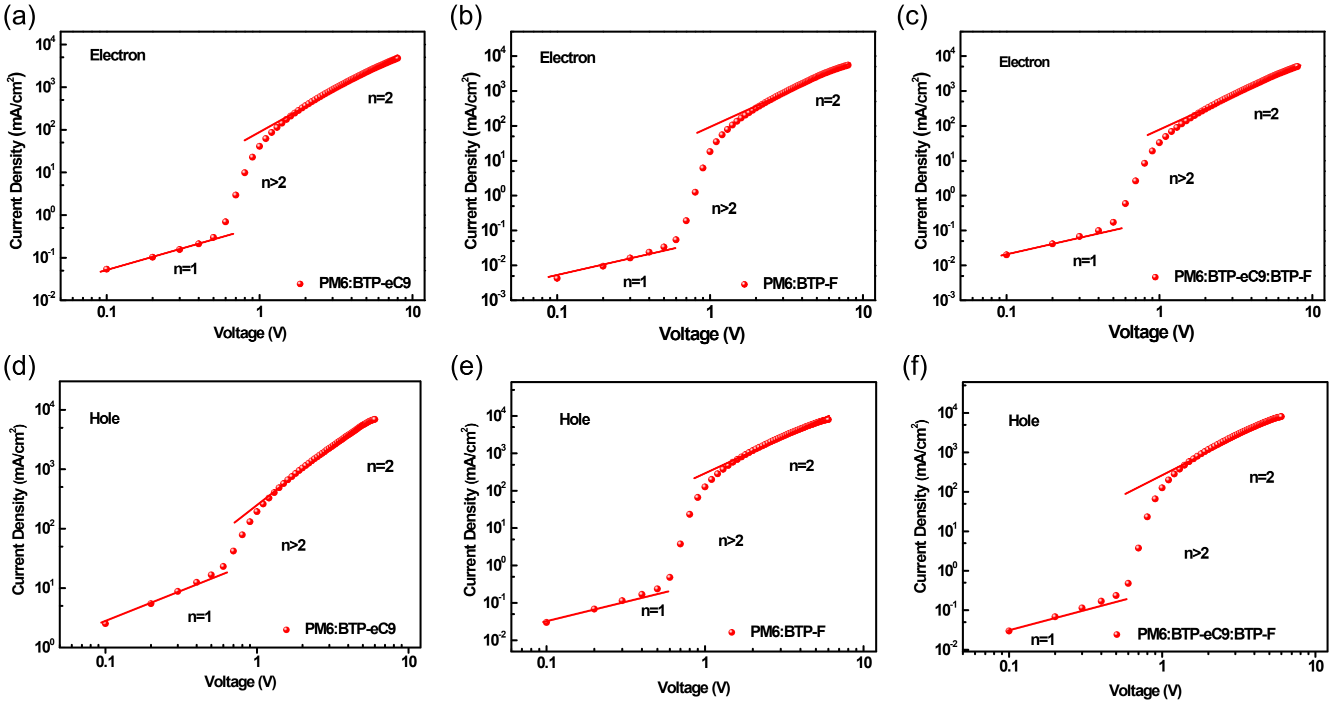

Fig. S9 *J-V* characteristics of (a-c) the hole-only devices, and (d-f) the electron-only devices based on different photovoltaic blends.

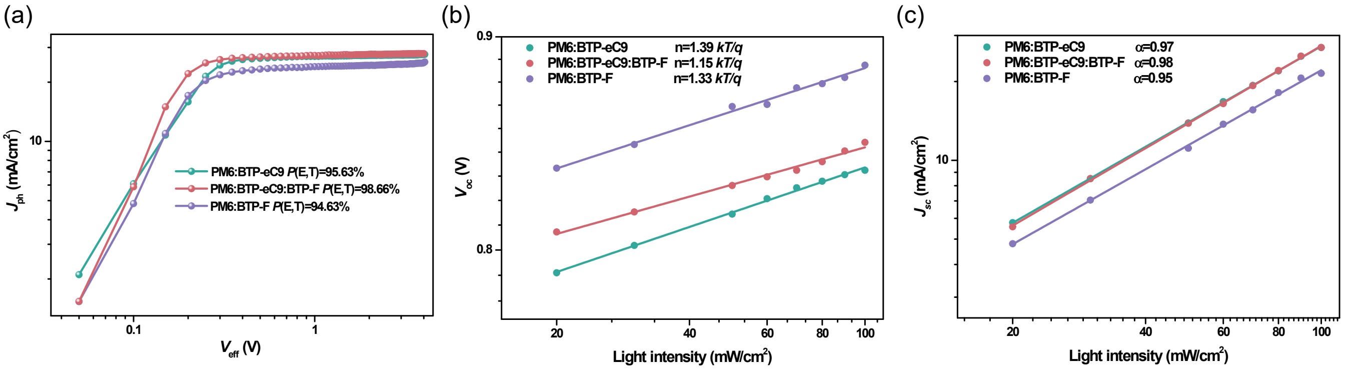

Fig. S10 (a) J_{ph} versus V_{eff} characteristics, (b) V_{oc} versus light intensity characteristics, and (c) J_{sc} versus light intensity characteristics of the binary and ternary OSCs.

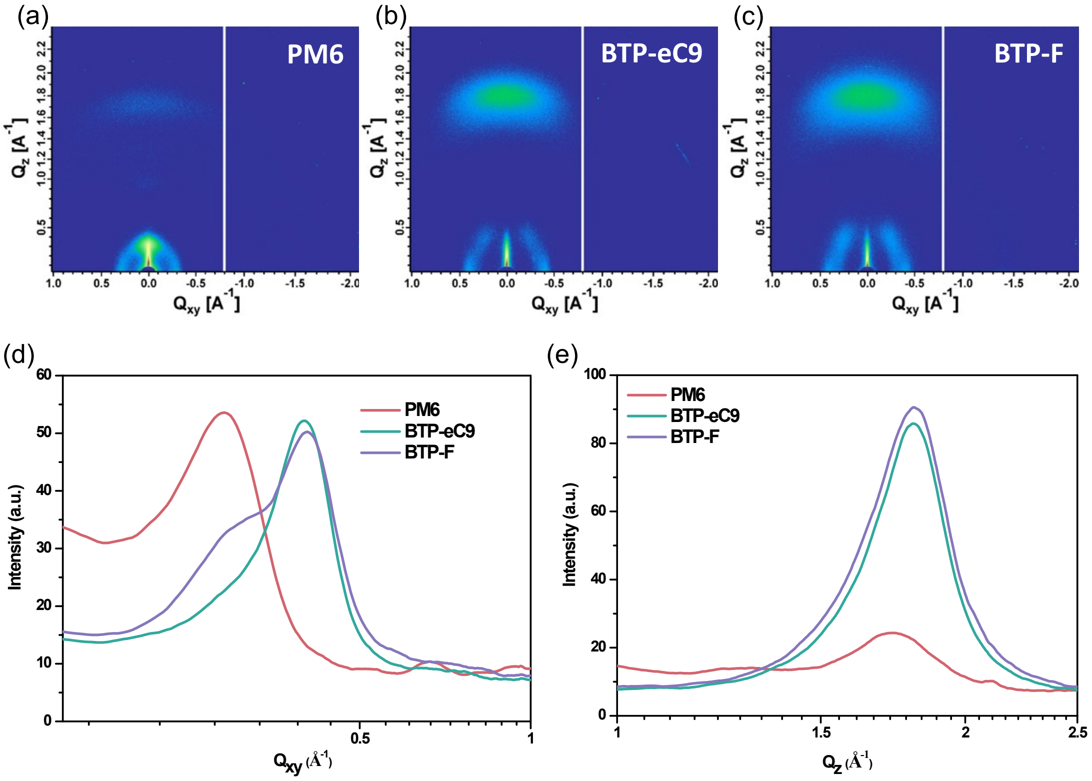

Fig. S11 (a-c) 2D GIWAXS patterns of PM6, BTP-eC9, BTP-F neat films and (d,e) the corresponding out-of-plane and in-plane line cuts.

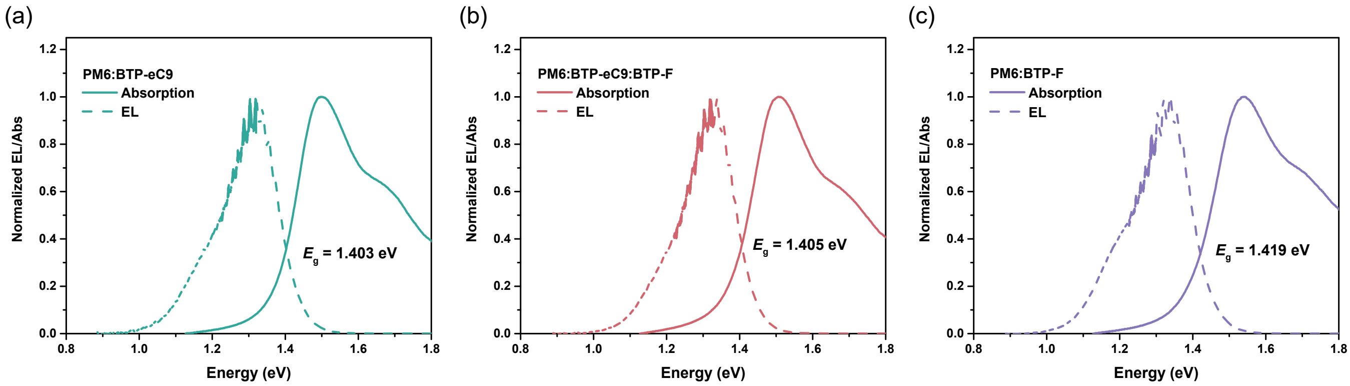

Fig. S12 Normalized absorption and electroluminescence spectra of (a) PM6:BTP-eC9, (b) PM6:BTP-eC9:BTP-F, and (c) PM6:BTP-F blends.

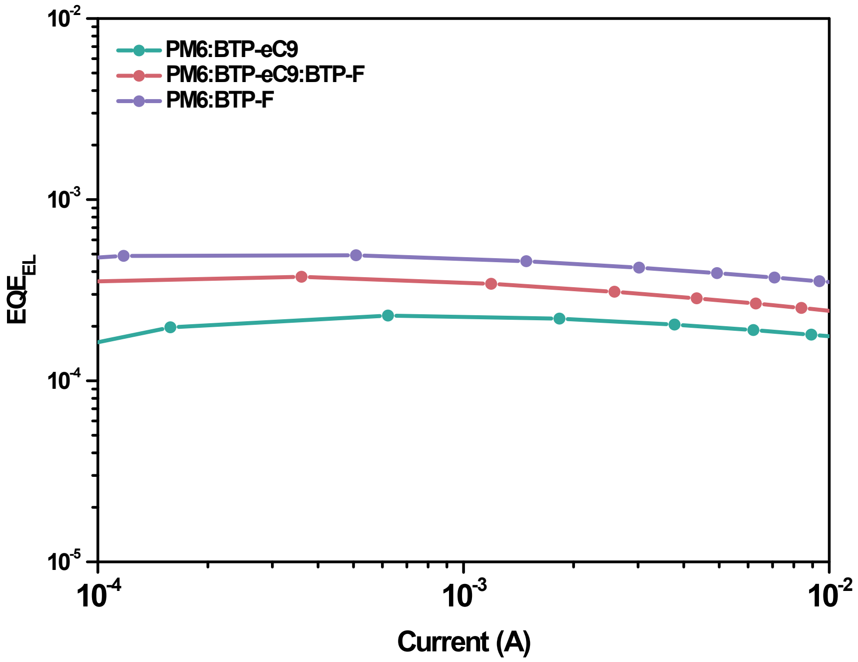

Fig. S13 The EQE_{EL} spectra of the binary and ternary devices.

Table S1 Device parameters of binary and ternary OSCs with different BTP-F contents.

BTP-F Contents	V_{oc} **[V]**	J_{sc} **[mA cm^{-2}]**	**FF [%]**	**PCE [%]**	**EQE (mA cm^{-2})**
0%	0.845	26.81	77.5	17.58	26.21
10%	0.854	26.88	78.7	18.07	26.42
15%	0.858	26.99	79.7	18.45	26.69
20%	0.858	26.81	77.5	17.83	26.20
100%	0.900	24.05	75.0	16.20	23.71

Table S2 Contact angle data using water and glycerol droplets and surface tension of PM6, BTP-eC9, and BTP-F.

Materials	θ_{water} **[°]**	$\theta_{glycerol}$ **[°]**	γ **[mN m^{-1}]**
PM6	103.3	91.3	17.18
BTP-eC9	94.5	81.3	23.58
BTP-F	94.6	78.9	26.51

Table S3 Device parameters for OSCs based on the selected Y-series acceptors.

Acceptors	**Donors**	**PCE (%)**	**Energy loss (V)**	**ΔV_{rad} (V)**	**$\Delta V_{\text{non-rad}}$ (V)**	**Ref.**
Y1	PBDB-T	13.4	0.57	0.27	0.25	6
Y2	PBDB-T	13.4	0.57	0.27	0.26	6
Y11	PM6	16.54	0.43	/	0.17	7
AQx1	PM6	13.3	0.52	0.26	0.21	8
AQx2	PM6	16.6	0.54	0.26	0.22	8
BTP-4F(Y6)	PM6	15.6	0.57	0.26	0.23	9
BTP-4Cl	PM6	16.5	0.53	0.26	0.21	9
BTP-eC7	PM6	6.94	0.56	0.263	0.225	10
BTP-eC9	PM6	17.8	0.56	0.263	0.227	3
BTP-eC11	PM6	16.9	0.55	0.262	0.229	3
Y18	PM6	16.5	0.52	0.27	0.21	11
BTP-C4C6-N	PM6	12.41	0.49	0.27	0.18	12
BTP-C2C4-N	PM6	10.3	0.52	0.27	0.21	12
BTP-C6C8-N	PM6	11.9	0.49	0.27	0.18	12
Y5	PM6	7.2	0.51	0.27	0.18	12
C6OB-H	PBDT-H	12.07	0.659	0.243	0.309	13
C6OB-H	PBDT-F	10.06	0.743	0.241	0.390	13
C6OB-F	PBDT-H	11.20	0.583	0.243	0.228	13
C6OB-F	PBDT-F	15.21	0.606	0.241	0.269	13
Y6	PBDB-TF	15.3	0.562	/	0.25	14
BTP-S1	PM6	15.21	0.56	0.27	0.22	15
BTP-S2	PM6	16.37	0.53	0.27	0.20	15
N3(As cast)	BT-2F	8.09	0.488	0.254	0.205	16
N3(TA)	BT-2F	14.66	0.508	0.253	0.226	16
N3(CS2)	BT-2F	15.39	0.534	0.256	0.244	16
Y6	D18	16.1	0.51	0.27	0.20	17
Y5	PM7	3.28	0.44	/	0.13	18
Y5	PM7:PBDB-T	5.27	0.47	/	0.16	18
Y5	PBDB-T	9.04	0.54	/	0.22	18
PYT	PBDBT	12.9	0.58	0.27	0.28	19
PZT	PBDBT	14.5	0.52	0.27	0.22	19
PZT-γ	PBDBT	15.8	0.51	0.26	0.22	19
BTP-eC9: BTP-F	PM6	18.45	0.466	0.268	0.198	**This Work**
BTP-F	PM6	16.20	0.451	0.266	0.185	**This Work**

References

1. C. Li, J. Zhou, J. Song, J. Xu, H. Zhang, X. Zhang, J. Guo, L. Zhu, D. Wei, G. Han, J. Min, Y. Zhang, Z. Xie, Y. Yi, H. Yan, F. Gao, F. Liu and Y. Sun, *Nat. Energy*, 2021, **6,** 605–613.
2. Y. Cai, Y. Li, R. Wang, Z. Chen, H. Wu, Y. Zhao, J. Zhang, Z. Ma, X. Hao, C. Zhang*, F. Huang, and Y. Sun, *Adv. Mater.* 2021, **3**, 2101733.
3. Y. Cui, H. Yao, J. Zhang, K. Xian, T. Zhang, L. Hong, Y. Wang, Y. Xu, K. Ma, C. An, C. He, Z. Wei, F. Gao and J. Hou, *Adv. Mater.*, 2020, **32**, 1908205.
4. J. Yuan, Y. Zhang, L. Zhou, G. Zhang, H.-L. Yip, T.-K. Lau, X. Lu, C. Zhu, H. Peng, P. A. Johnson, M. Leclerc, Y. Cao, J. Ulanski, Y. Li and Y. Zou, *Joule*, 2019, **3**, 1140.
5. M. Zhang, M. Zeng, L. Ye, S. Tan, B. Zhao, H. S. Ryu, H. Y. Woo and Y. Sun, *Solar Energy*, 2020, **208**, 866-872.
6. J. Yuan, T. Huang, P. Cheng, Y. Zou, H. Zhang, J. L. Yang, S. Y. Chang, Z. Zhang, W. Huang, R. Wang, D. Meng, F. Gao and Y. Yang, *Nat. Commun.*, 2019, **10**, 570.
7. S. Liu, J. Yuan, W. Deng, M. Luo, Y. Xie, Q. Liang, Y. Zou, Z. He, H. Wu and Y. Cao, *Nat. Photonics*, 2020, **14**, 300-305.
8. Z. Zhou, W. Liu, G. Zhou, M. Zhang, D. Qian, J. Zhang, S. Chen, S. Xu, C. Yang, F. Gao, H. Zhu, F. Liu and X. Zhu, *Adv. Mater.*, 2020, **32**, e1906324.
9. Y. Cui, H. Yao, J. Zhang, T. Zhang, Y. Wang, L. Hong, K. Xian, B. Xu, S. Zhang, J. Peng, Z. Wei, F. Gao and J. Hou, *Nat. Commun.*, 2019, **10**, 2515.
10. L. Hong, H. Yao, Z. Wu, Y. Cui, T. Zhang, Y. Xu, R. Yu, Q. Liao, B. Gao, K. Xian, H. Y. Woo, Z. Ge and J. Hou, *Adv. Mater.*, 2019, **31**, e1903441.
11. C. Zhu, J. Yuan, F. Cai, L. Meng, H. Zhang, H. Chen, J. Li, B. Qiu, H. Peng, S. Chen, Y. Hu, C. Yang, F. Gao, Y. Zou and Y. Li, *Energy Environ. Sci.*, 2020, **13**, 2459-2466.
12. J. Pan, Y. Shi, J. Yu, H. Zhang, Y. Liu, J. Zhang, F. Gao, X. Yu, K. Lu and Z. Wei, *ACS Appl. Mater. Interfaces*, 2021, **13**, 22531-22539.
13. G. U. Kim, C. Sun, J. S. Park, H. G. Lee, D. Lee, J. W. Lee, H. J. Kim, S. Cho, Y. H. Kim, S. K. Kwon and B. J. Kim, *Adv. Funct. Mater.,* 2021, **31**, 2100870.
14. R. Yu, H. Yao, Y. Cui, L. Hong, C. He and J. Hou, *Adv. Mater.*, 2019, **31**, 1902302.
15. S. Li, L. Zhan, Y. Jin, G. Zhou, T. K. Lau, R. Qin, M. Shi, C. Z. Li, H. Zhu, X. Lu, F. Zhang and H. Chen, *Adv. Mater.*, 2020, **32**, 2001160.
16. J. Ge, L. Hong, W. Song, L. Xie, J. Zhang, Z. Chen, K. Yu, R. Peng, X. Zhang and Z. Ge, *Adv. Energy Mater.*, 2021, **11,** 2100800.
17. J. Hofinger, C. Putz, F. Mayr, K. Gugujonovic, D. Wielend and M. C. Scharber, *Mater. Adv.*, 2021, **2,** 4291-4302.
18. H. Liu, M. Li, H. Wu, J. Wang, Z. Ma and Z. Tang, *J. Mater. Chem. A*, 2021. https://doi.org/10.1039/D1TA00576F.
19. H. Fu, Y. Li, J. Yu, Z. Wu, Q. Fan, F. Lin, H. Y. Woo, F. Gao, Z. Zhu and A. K. Jen, *J. Am. Chem. Soc.*, 2021, **143**, 2665.